As-Cast Microstructures of High Entropy Alloys Designed to Be TaC-Strengthened

Patrice Berthod

BILINGUAL PUBLISHING CO.
Pioneer of Global Academics Since 1984

Journal of Metallic Material Research
https://ojs.bilpublishing.com/index.php/jmmr

ARTICLE

As-Cast Microstructures of High Entropy Alloys Designed to Be TaC-Strengthened

Patrice Berthod[1,2*]

1. Faculty of Sciences and Technologies, University of Lorraine, Vandoeuvre-lès-Nancy, 54500, France
2. Institut Jean Lamour, CNRS, Nancy, 54000, France

ARTICLE INFO

Article history
Received: 5 May 2022
Revised: 30 May 2022
Accepted: 1 June 2022
Published Online: 6 June 2022

Keywords:
HEA alloys
TaC carbides
As-cast microstructures
Hardness

ABSTRACT

In this work two new alloys were obtained by extrapolation from a well-known high entropy alloy, the equimolar CoNiFeMnCr one. This was done by the addition of carbon and of tantalum, Ta being one of the strongest MC-former elements. They were produced by conventional casting under inert atmosphere. The obtained microstructures were characterized by X-ray diffraction, metallography, electron microscopy, and energy dispersion spectrometry. Their hardness was also measured by hardness indentation. In parallel, the original CoNiFeMnCr alloy was also synthesized and characterized for comparison. The reference HEA alloy is single-phased with an austenitic structure, while the two {Ta, C}-added alloys are double-phased, with an austenitic matrix and interdendritic script-like TaC carbides. The matrixes of these HEA/TaC alloy are equivalent to an equimolar CoNiFeMnCr alloy to which 2 wt.% Ta is present in solid solution. The presence of the TaC carbides caused a significant increase in hardness which suggests that the HEA/TaC alloys may be mechanically stronger than the HEA reference alloy at high temperature.

1. Introduction

The past decade has seen the appearance of a new generation of alloys interesting for various uses needing high mechanical properties: the "high entropy alloy" principle (HEA). Since some of them can offer good general properties at high temperatures, they may compete with the superalloys which are used for a long time in the aeronautic industry (turbine disks and blades, for instance), power generation (burners, hottest parts of turbines…) and industrial processes working at elevated temperature (tools for shaping molten glasses…) [1-3]. Many HEAs contain in equimolar quantities (or also in various quantities) and with different numbers of metals often belonging to the {Fe, Co, Ni, Cr, Mn} list [4,5]. These five elements constitute a quinary system, the thermodynamic description of which was studied until recently [6,7]. Beside the conventional foundry of equimolar FeCoNiCrMn alloys, different

*Corresponding Author:
Patrice Berthod,
Faculty of Sciences and Technologies, University of Lorraine, Vandoeuvre-lès-Nancy, 54500, France; Institut Jean Lamour, CNRS, Nancy, 54000, France;
Email: patrice.berthod@univ-lorraine.fr

DOI: https://doi.org/10.30564/jmmr.v5i2.4685

ways of elaboration of superalloys were recently applied to HEAs: single crystalline growth [8], additive manufacturing [9] or thin film deposition [10]. Their behaviors in case of extreme conditions of solicitations were also explored, mechanical properties [11,12] or chemical reactivity at high temperature [13]. Evolutions of chemical composition - variation of the Co or Ni content [14] (and even suppression of Co [15] or of Ni [16]) - were tested, and the notion of "Medium Entropy Alloys" has also appeared [17]. Nanoparticles of SiC particles have also started to be introduced in HEAs [18].

The equimolar FeCoNiCrMn alloys are not far from cobalt-based superalloys, strengthened by solid solution, or from the matrix of polycrystalline cobalt-based superalloys with grain boundaries strengthened by carbides. Indeed, these cobalt-based superalloys are generally rich in nickel and in chromium, at least. The contents are not equivalent (50 wt.% Co or a little more, 10 wt.% Ni and 30 wt.% Cr) but one can guess that HEAs involving these elements may usefully contain primary chromium carbides or MC carbides as additional phases. The additional presence of such second phase (and third phase in some cases) is likely to push upwards the mechanical resistance at high temperature of HEAs, the matrix intrinsic strength of which can become no longer sufficient. A particular beneficial effect can be expected from the use of TaC carbides earlier successfully tested in polycrystalline chromia-forming cobalt-based model or industrial alloys [19,20].

The aim of this work is to start investigating the principle of {*in situ* precipitated}-interdendritic script-like MC carbides, by synthetizing several HEA-based alloys in which the formation of MC carbides is promoted by the addition of carbon and of Ta, in quantities having earlier led to MC populations in adequate fractions [19,20]. Checking the reproduction of alloys similar to the model alloys cited above but with a matrix equivalent to a HEA, and characterizing their as-cast microstructures as well as their room temperature hardness, are the objectives of this work.

2. Materials and Methods

The three alloys were prepared by mixing pure elements: Co (centimetric flakes), Ni (millimetric balls), Fe (centimetric flakes), Mn (centimetric flakes) and Cr (centimetric blocks) for the "HEA" alloy, with additionally C (millimetric graphite rods) and Ta (millimetric slugs). The purity of all elements was > 99.9 wt.% (Alfa Aesar and Aldrich). The charges were weighed with accuracy to reach 40 g and the following contents:

- Equimolar CoNiFeCrMn, alloy called "HEA ref.";
- 96 wt.% (CoNiFeCrMn) - 0.25 wt.% C - 3.72 wt.% Ta, alloy called "HEA/TaC1";
- 92 wt.% (CoNiFeCrMn) - 0.50 wt.% C - 7.44 wt.% Ta, alloy called "HEA/TaC2".

Each mix of elements was placed in a copper crucible equipping a high frequency induction furnace (CELES, France; power: 50 kW). This metallic crucible was continuously cooled by circulating water at ambient temperature during the elaboration steps.

After introduction of the mix of pure elements, a silica tube was placed around the crucible and closed to allow the evacuation of the present air, operated by pumping. Crucible and silica tube were surrounded by a water-cooled copper coil in which an alternative current circulated. The frequency of the alternative current was between 100 kHz and 150 kHz, and the applied voltage was between 4 kV and 5 kV, this depending on the alloy. After 3 cycles made of pumping until 4×10^{-5} bars followed by filling by pure Argon, the internal atmosphere was considered as being pure Ar, with a pressure rated at about 400 mbars.

Heating led to the melting of the charges made of pure elements, and the obtained liquid alloy was maintained at the highest reached temperature during fifteen minutes to achieve total melting and chemical homogeneity for the liquid. During the cooling, produced by decreasing the input power/voltage, the alloys started solidifying, and later cooled in solid state. After about 20 minutes to 30 minutes, the obtained ingots were again at room temperature and they were extracted from the crucible.

Each ingot was first embedded in a cold resin mixture (ESCIL, France) to be more easily cut using a metallographic saw to produce a sample with the adequate shape and size to prepare a metallographic sample. The cut part was embedded in the cold {resin + hardener} mixture. The obtained embedded alloy samples were ground by using first #600-grade SiC papers, and second #1200-grade papers. Final polishing was carried out using a textile disk enriched with 1 μm hard particles.

The obtained mirror-like samples were put, one after one, in the chamber of a Scanning Electron Microscope/SEM, model JSM-6010LA (JEOL, Japan). Their microstructures were observed in Back Scattered Electrons mode/BSE (acceleration voltage: 15 kV), at different magnifications. The Image J software was used to measure the surface fractions of the present particles (on three × 1000 SEM/BSE images per alloy). Energy Dispersive Spectrometry was used to control the obtained chemical compositions by full frame analysis (at the × 250 magnification). Additionally, spot analyses were performed on the visible particles to identify them and to specify the chemical composition of the matrix. X-ray diffraction/XRD was

also carried out for all alloys to complete the identification of the present phases. This was done using a D8 Advance diffractometer from Bruker (wavelength of the Kα transition of Cu).

The metallographic samples were also subjected to indentation tests to assess the hardness of all alloys. This was carried out using an automatic indentation machine (PRESI, France), according to the Vickers method. The applied load was 10 kg for all tests. Five indentations were carried out per alloy.

3. Results

3.1 Microstructure and Composition of the "HEA ref." Alloy

X-ray diffraction (XRD) carried out on the reference alloy designed to be CoNiFeMnCr equimolar led to the diffractogram given in Figure 1. This one demonstrates that the alloy is single-phased and contains only a Face Centered Cubic solid solution. This is confirmed by the observation of the microstructure of the metallographic sample using the SEM in BSE mode, illustrated by the SEM/BSE micrograph provided in Figure 2 together with an EDS spectrum showing the peaks of the elements present in the alloy. The alloy effectively appears as single-phased while the EDS results (Table 1 and Table 2) confirm that the alloy is really equimolar.

Table 1. Chemical composition in weight percent of the reference alloy (average and standard deviation calculated from the results of three × 250 full frame areas)

HEA ref. Whole alloy	Wt.% Co	Wt.% Ni	Wt.% Fe	Wt.% Mn	Wt.% Cr	
Average content	19.8	21.4	19.5	19.5	19.8	
Standard deviation	0.2	0.2	0.1	0.0	0.1	

Table 2. Chemical composition in atomic percent of the reference alloy (average and standard deviation calculated from the results of three × 250 full frame areas)

HEA ref. Whole alloy	At.% Co	At.% Ni	At.% Fe	At.% Mn	At.% Cr	
Average content	18.9	20.4	19.5	19.9	21.3	
Standard deviation	0.1	0.2	0.1	0.0	0.1	

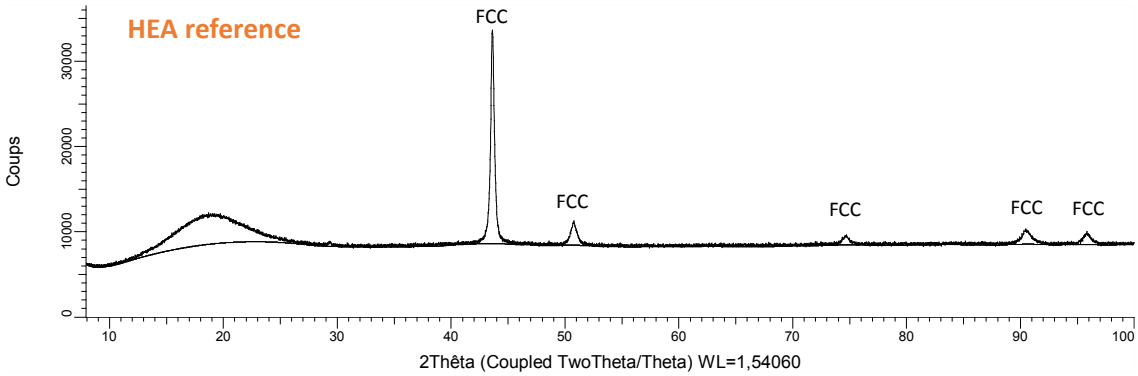

Figure 1. Diffractogram of the HEA reference alloy

(peaks indexed by "FCC": Face Centered Cubic crystalline network of the single phase)

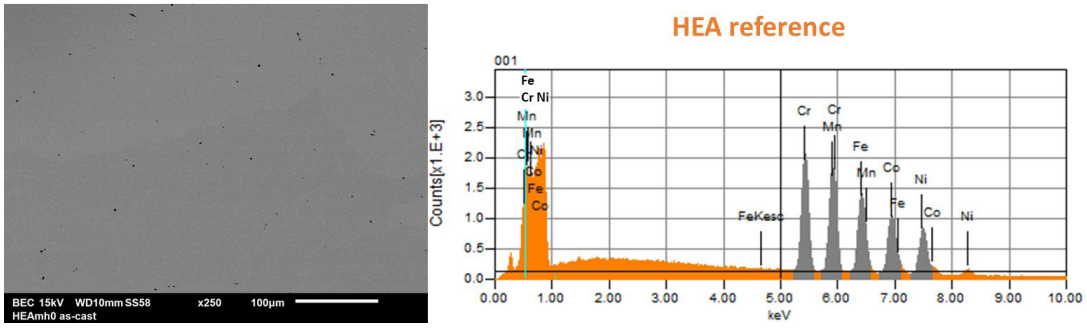

Figure 2. SEM/BSE micrograph of the microstructure of the HEA reference alloy (left) and EDS spectrum acquired on this area (right)

An elemental map was also acquired on the HEA reference alloy to study its chemical homogeneity (Figure 3). It allows observing that all elements are rather homogeneously distributed in the single phase, except manganese which is more present in areas looking as interdendritic spaces.

3.2 Microstructures and Compositions of the {Ta,C}-Containing Alloys

The X-ray diffractograms are acquired on the two alloys resulting from the addition of tantalum and carbon (Figure 4) both contain all the peaks corresponding to the FCC solid solution CoNiFeMnCr already featuring in the diffractogram of the HEA reference alloy (Figure 1). Additional peaks are also present: they correspond to the TaC phase. The microstructures of these two {Ta, C}-containing alloys are illustrated by SEM/BSE micrographs in Figure 5 together with the EDS spectra acquired on these zones. The global chemical compositions of these two alloys measured by full frame EDS analysis on three distinct zones (magnification × 250) and the chemical composition of the matrix measured by spot analysis in three distinct locations, are given in Table 3 for the HEA/TaC1 alloy and in Table 4 for the HEA/TaC2 alloy. Obviously the two alloys each contain at least two phases, including a dendritic matrix. The global chemical compositions are globally well respected.

The microstructure of the HEA/TaC1 alloy is composed of a dendritic matrix and of an interdendritic compound. Observations at higher magnification (Figure 6, left) allow distinguishing two phases in the interdendritic compound. This compound is made of a part of matrix (identified by EDS spot analysis) and of white particles. These ones are TaC carbides, the presence of which was already shown by XRD. The TaC composition was evidenced by spot EDS analysis performed on the coarsest white particles found: almost exclusive presence of Ta and C, and molar equivalence between Ta and C. Due to its interdendritic location and to its constitution in two phases closely imbricated, this compound is certainly of a eutectic nature; it precipitated at the end of solidification with the simultaneous growth of additional matrix and TaC carbides.

Although similar to the HEA/TaC1 one (presence of a dendritic matrix, {matrix + TaC} compound), the microstructure of the HEA/TaC2 alloy presents a particularity since it also contains in addition blocky white particles. EDS spot analysis shows that there are also TaC carbides.

The surface fractions of the TaC phase were measured on three randomly chosen × 1000 SEM/BSE micrographs for the two alloys, using the Image J software, after having rated the threshold to isolate the white TaC from the gray matrix. The HEA/TaC1 alloy contains about 6.4 surf.% of TaC and the HEA/TaC2 contains 11.2 surf.% TaC (average values).

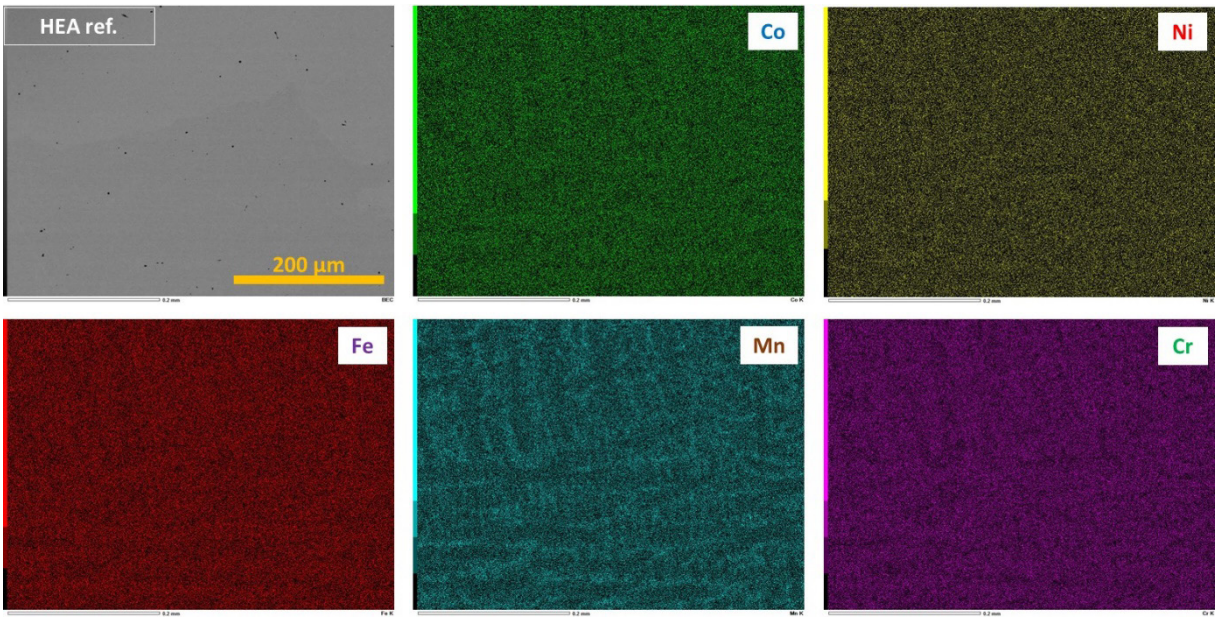

Figure 3. X-maps obtained on the HEA reference

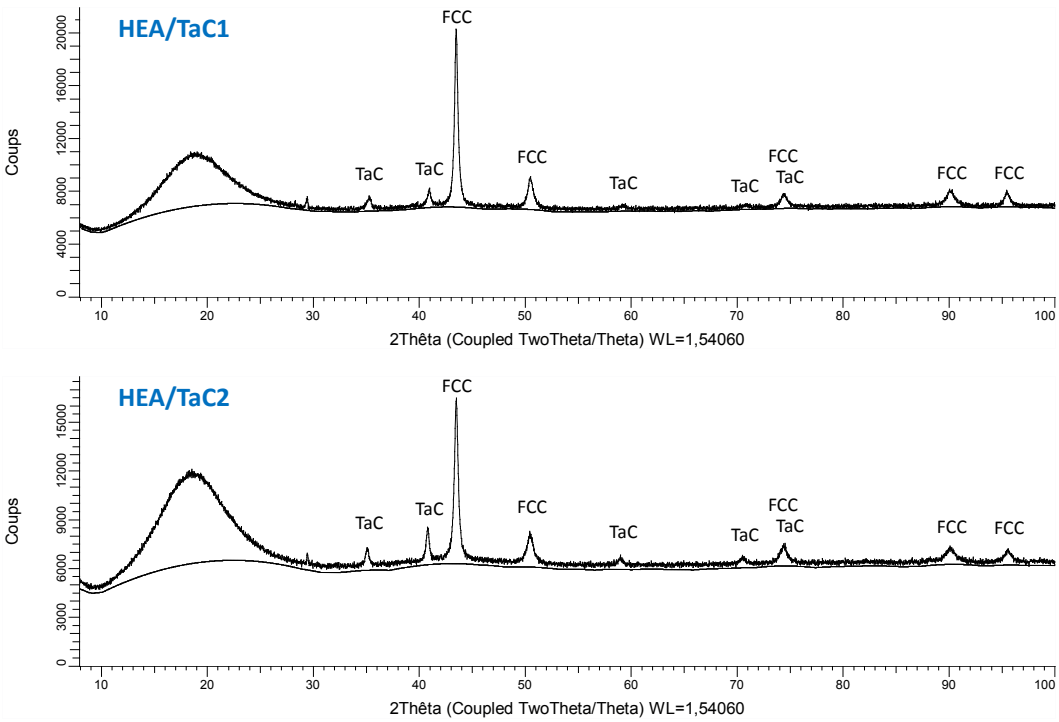

Figure 4. Diffractograms of the HEA/TaC1 (top) and HEA/TaC2 (bottom) alloys

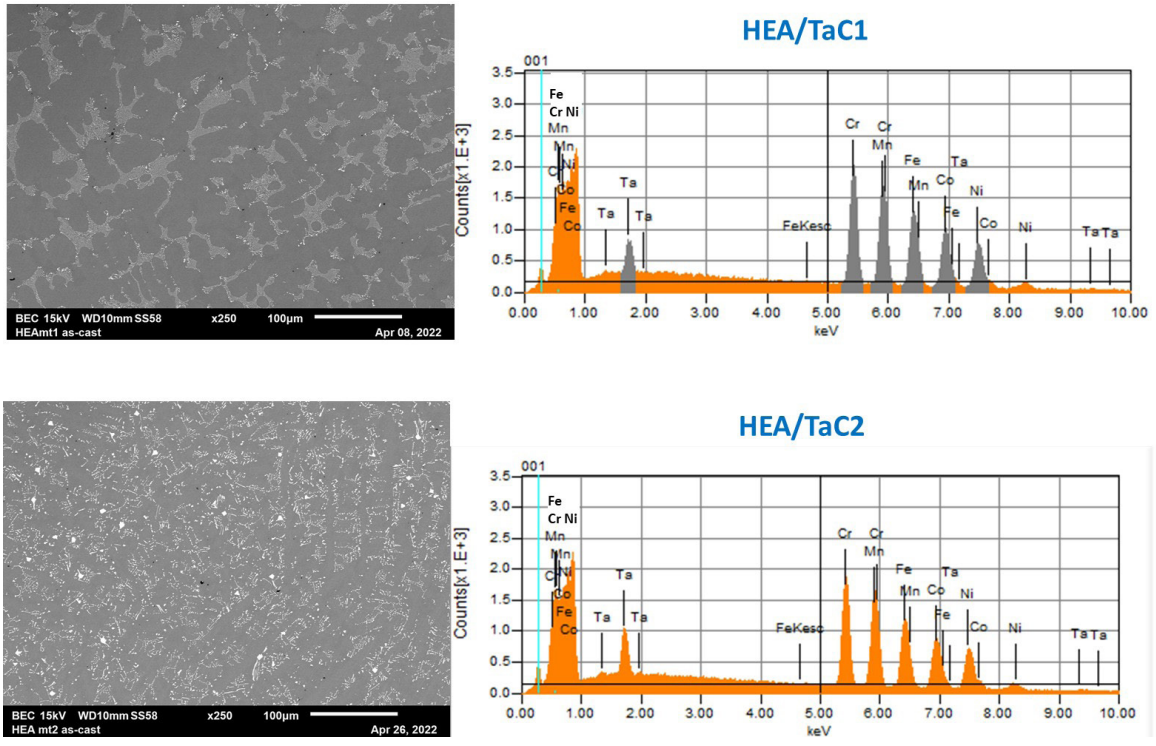

Figure 5. SEM/BSE micrographs of the microstructure of the HEA/TaC1 alloy (top, left) and EDS spectrum acquired on this area (top, right), and of the HEA/TaC2 alloy (bottom left) and the corresponding EDS spectrum (bottom, right)

Table 3. General chemical compositions of the HEA/TaC1 alloy (average and standard deviation calculated from the results of three × 250 full frame areas) and chemical compositions of its matrix (all contents in weight percent, carbon not possible to analyze but supposed to be well respected: 0.25 wt.% C)

HEA/TaC1 Whole alloy	Wt.% Co	Wt.% Ni	Wt.% Fe	Wt.% Mn	Wt.% Cr	Wt.%Ta
Average content	19.3	20.1	18.6	18.3	19.2	4.5
Standard deviation	0.2	0.5	0.5	0.3	0.3	0.4
HEA/TaC1 Matrix	**Wt.% Co**	**Wt.% Ni**	**Wt.% Fe**	**Wt.% Mn**	**Wt.% Cr**	**Wt.%Ta**
Average content	20.5	20.5	20.9	16.7	19.4	2.1
Standard deviation	0.4	0.3	0.9	1.4	0.6	0.1

Table 4. General chemical compositions of the HEA/TaC2 alloy (average and standard deviation calculated from the results of three × 250 full frame areas) and chemical compositions of its matrix (all contents in weight percent, carbon not possible to analyse but supposed to be well respected: 0.5 wt.% C)

HEA/TaC2 Whole alloy	Wt.% Co	Wt.% Ni	Wt.% Fe	Wt.% Mn	Wt.% Cr	Wt.TaC
Average content	18.5	20.0	17.9	18.1	19.1	6.3
Standard deviation	0.5	0.2	0.5	0.2	0.3	0.7
HEA/TaC2 Matrix	**Wt.% Co**	**Wt.% Ni**	**Wt.% Fe**	**Wt.% Mn**	**Wt.% Cr**	**Wt.%TaC**
Average content	18.2	22.8	16.2	22.1	18.9	1.9
Standard deviation	0.5	1.2	2.1	2.0	0.3	0.4

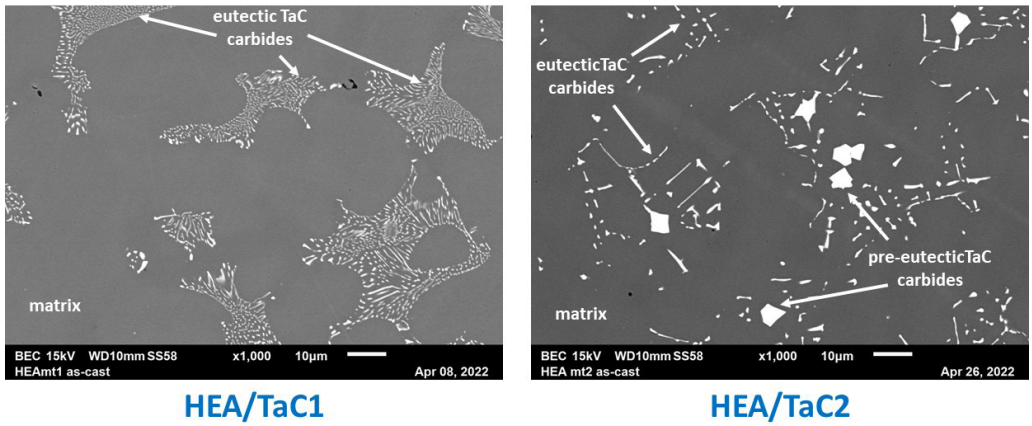

Figure 6. High magnification SEM/BSE micrographs for observation in details of the microstructures of the two {Ta, C}-containing HEA alloys (left: HEA/TaC1, right: HEA/TaC2)

Several EDS spot analyses were also carried out in the matrixes of both alloys (bottom parts of Table 3 and Table 4). Unsurprisingly (since there is only a second phase which is TaC carbide in both alloys), the matrixes are equimolar in Co, Ni Fe, Mn and Cr. But they also contain about 2 wt.% Ta, showing that only a part of tantalum is involved in carbides. A part of carbon is consequently also necessarily present in solid solution in the matrix but, unfortunately, it cannot be analyzed.

One can also notice that the Mn and Fe contents seem varying in the matrix of each alloy. The X-maps presented in Figure 7 effectively evidences in the case of the HEA/TaC1 alloy, slight but real variations in Mn content in its matrix. One encounters again what was observed in the HEA ref. alloy in Figure 3.

3.3 Hardness of the HEA ref. and HEA/TaC Alloys

Per alloy, five indentations were carried out according to the Vickers method, with a 10 kg load. The results, displayed in Table 5, are available for comparison with the hardness of the HEA reference alloy. It clearly appears that the presence of carbides induced a significant increase in hardness.

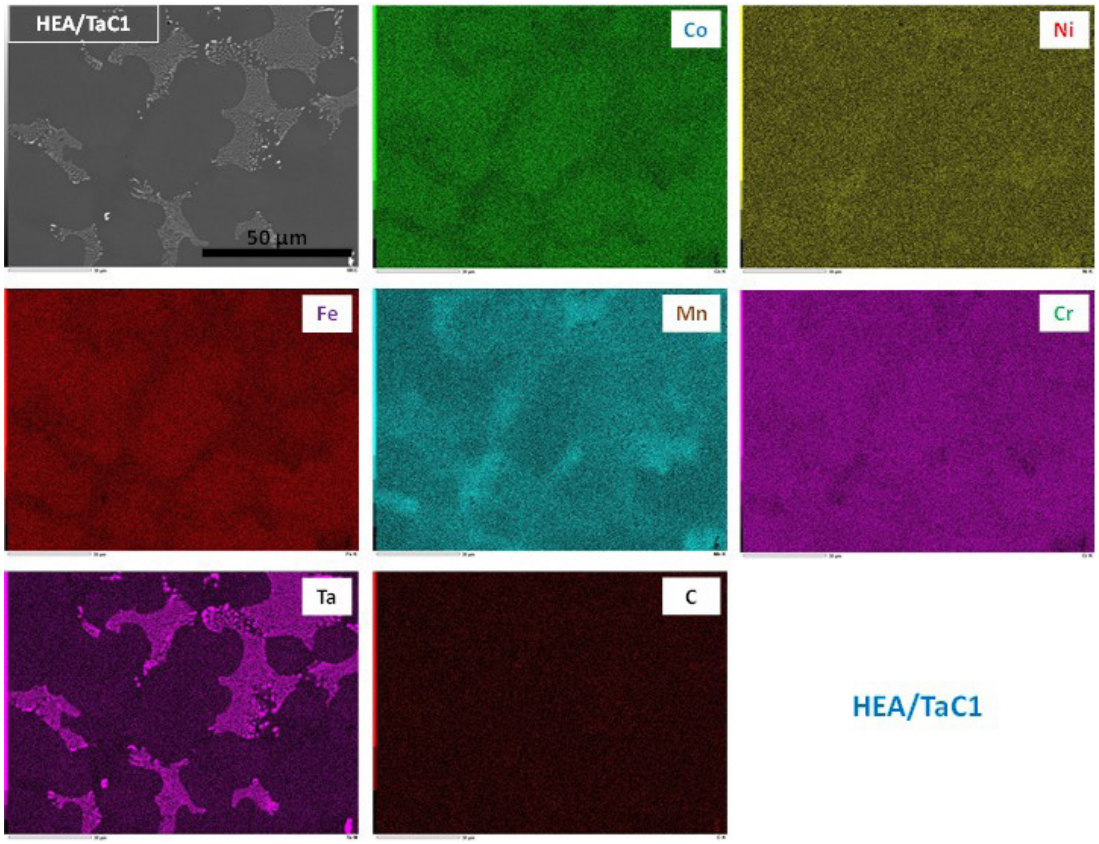

Figure 7. X-maps obtained on the HEA/TaC1 alloy

Table 5. Hardness of the HEA/TaC alloys in comparison with the HEA reference alloy

Vickers 10 kg 5 indent.	HEA ref.	HEA/TaC1	HEA/TaC2
Average content	121	180	194
Standard deviation	2	4	5

4. Discussion

The first alloy to be produced with the apparatus used here (High Frequency Induction furnace, fusion and solidification achieved in a unique water-cooled copper crucible) and the elaboration protocol (all the operating parameters applied here) was the HEA ref. one. It was successfully obtained as a single-phased austenitic alloy, as it is obtained by all researchers working on this type of HEA alloy. The elemental distribution was globally homogeneous, except concerning Mn. The two HEA/TaC alloys themselves presented a matrix globally homogeneous, except Mn again. In their case, the presence of interdendritic particles allowed evidencing that the Mn-enriched zones of the matrix were close to the interdendritic spaces, and thus that Mn was subjected to positive segregation. The knowledge of this not perfect chemical homogeneity of the matrix allows thinking to apply a homogenization heat treatment prior to the use of these alloys, since this small lack of homogeneity can be deleterious for some properties.

The addition of Ta and of C successfully led to an interesting population of carbides. TaC formed at the expense of other types of carbides, notably at the expense of chromium carbides as this previously occurred in earlier alloys fabricated following the same elaboration way and similar protocols (in Ni-30Cr-0.2 or 0.4C-3 or 6Ta [21]). In that way, the 20 wt.% Ni in presence of 20 wt.%Cr is probably compensated by the 20 wt.% Co and 20 wt.% Fe more favorable to the formation of TaC. Indeed, these two last elements did not cause earlier problem of predominance of chromium carbides on TaC carbides in Cr-rich alloys for which they were the base elements [22-24].

As in the earlier studied Cr-rich alloys based on Co [22] or on Fe [23,24], the TaC carbides obtained here have appeared in the last zones to solidify and they are essentially eutectic with close imbrication with matrix, and of the script-like morphology. Good initial interdendrites and intergrains cohesion at high temperature can be thus expected on long time for delaying the transition from secondary state of creep to the tertiary state. It is true that other TaC particles - coarse blocky carbides not mixed with matrix - are present in the HEA/TaC2 alloy, but one can think that they can be not detrimental for the mechanical properties at high temperatures. These blocky TaC are similar to the ones previously observed in cobalt-chromium alloys with high contents in Ta en C (15 wt.% and 1 wt.% C) earlier studied [25]. In these alloys earlier studied, thermodynamic calculations evidence that low C and Ta contents led to the appearance of eutectic TaC carbides only, the dendritic matrix being thus the first solid phase to crystallize from the liquid state. In contrast, higher C and Ta contents induced the pre-eutectic crystallization of a first TaC population instead of the matrix. These pre-eutectic TaC carbides grew, freely in the liquid, with a blocky and angular shape and became the coarse carbides not necessarily located in the interdendritic spaces observed in the metallographic samples. The origin of the blocky carbides observed in the HEA/TaC2 alloy is certainly the same: moving from {0.25 wt.% C, 3.7 wt.% Ta} to {0.50 wt.% C, 7.4 wt.% Ta} obviously induced here too change of location of the alloy from one side of the eutectic valley to the other side, with as consequence a solidification of first TaC and second TaC & matrix, instead a solidification of first matrix and second TaC & matrix. By comparison with these earlier studied cobalt-based alloys, the replacement of a great part of cobalt by new elements to achieve equal proportions in Co, Ni, Fe, Cr and Mn, has obviously caused a displacement of the eutectic valley toward lower tantalum and carbon contents.

To speak again about the matrix, this one is not really an equimolar alloy since it contains also 2 wt.% Ta. This is the typical Ta content in the matrix of Cr-rich Co-based alloys containing 0.2C-3Ta or 0.4C-6Ta (wt.%) [22] (and twice the one in the Cr-rich Fe-based alloys with the same C and Ta contents [23], or half the one in the Cr-rich Fe-based alloys with the same C and Ta contents [21]). The presence of Ta in solid solution in the matrix did not change its single-phase state and it may possibly bring an additional strengthening.

Concerning the properties of these TaC-strengthened alloys at high temperature, an ongoing study has brought first results of microstructure behavior. They are illustrated in Figure 8. After 50 h at 1100 °C, no start of local melting was detected. Furthermore, the TaC carbides population has not significantly changed. The script-like shape of the eutectic carbides is kept, despite a limited fragmentation and the pre-eutectic blocky carbides of the HEA/TaC2 alloy are not affected. There is another modification which is interesting to notice: the precipitation of fine carbides from the Ta and C initially present in solid solution in the matrixes of the as-cast alloys. This is a potential source of additional strengthening which can be useful during the steady state of creep deformation (secondary step of creep). These secondary TaC are more numerous in the HEA/TaC1 alloy than in the HEA/TaC2 alloy. In this second alloy, the higher density of primary TaC led Ta and C diffusing towards the neighbor carbides to precipitate on their surfaces. The contribution of fine dispersed TaC carbides will be thus more useful for the HEA/TaC1 alloy than for the other alloy. Creep tests are scheduled on these HEA/TaC1 and HEA/TaC2 alloys to assess the progress

in strength at high temperature due to these TaC carbides added to the HEA reference alloy.

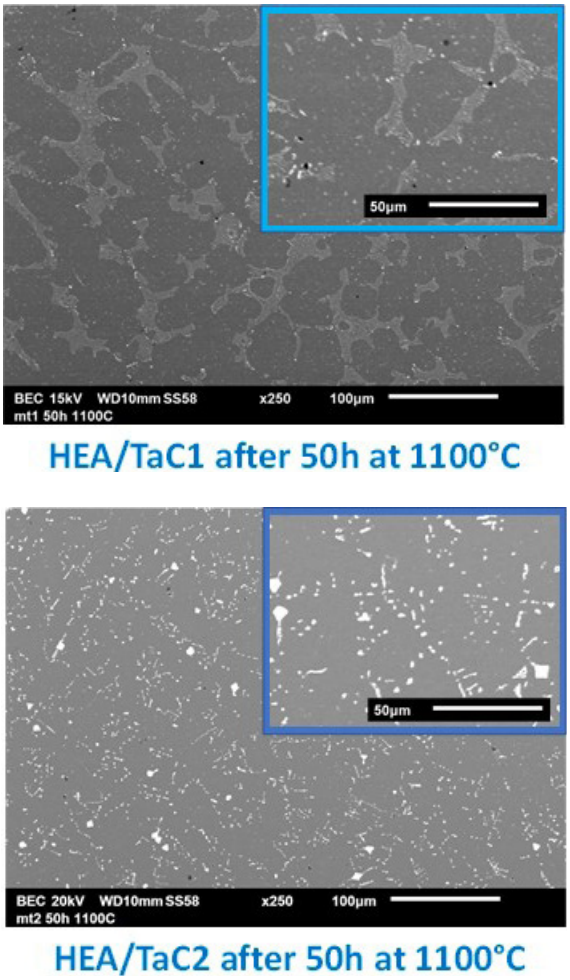

Figure 8. Microstructures of the two HEA/TaC1 (left) and HEA/TaC2 (right) alloys after 50 hours at 1100 °C (SEM/BSE at the × 250 magnification and at × 500 in the top right corners).

5. Conclusions

The as-cast microstructures obtained for the new alloys resulting from the addition of Ta and C to an equimolar CoNiFeMnCr HEA alloy are thus composed of a matrix similar to a HEA alloy, despite the presence of Ta (and C) in solid solution in proportion much lower than the first five elements, and of interdendritic TaC carbides forming a eutectic compound with the peripherical parts of the matrix dendrites. The combination of these two phases can be potentially very interesting, knowing the good properties of equimolar CoNiFeMnCr alloys (furthermore possibly enhanced by Ta in solid solution) and the script-like TaC carbides which have earlier demonstrated their beneficial effect for the creep resistance of Cr-rich Co-based superalloys. Now, the morphological sustainability of the script-like TaC carbides on long term at high temperature needs to be tested, and the mechanical properties are to be tested in hot conditions, by creep tests for instance. Another important point to check is the behavior of these HEA/TaC alloys in oxidation at high temperature. This one risks to be not sufficient because of the rather low chromium content to which the equimolar criterion led. These investigations of the microstructure, mechanical and oxidation properties at high temperature are being done in new ongoing studies.

Author Contributions

This present study is the own work of the single author.

Conflict of Interest

There is no conflict of interest for this work.

Funding

This research received no external funding.

Acknowledgments

To Ghouti Medjahdi, member of the CC X-Gamma service of the Jean Lamour Institute, for his help for the X-ray diffraction runs,

To Erwan Etienne, member of the CC 3M service of the Jean Lamour Institute, for his technical help for the indentation tests.

References

[1] Chester, T.S., Hagel, W.C., 1972. The Superalloys-Vital High Temperature Gas Turbine Materials for Aerospace and Industrial Power. John Wiley & Sons: New York.

[2] Sims, C.T., Stoloff, N.S., Hagel, W.C., 1987. Superalloys II. High: Temperature materials for aerospace and industrial power. John Wiley & Sons: New York.

[3] Kracke, A., Allvac, A., 2010. Superalloys, the most successful alloy system of modern times-past, present and future. Proceedings of the 7th International Symposium on Superalloy. 718, 13-50.

[4] Liu, S.F., Wu, Y., Wang, H.T., et al., 2018. Stacking fault energy of face-centered-cubic high entropy alloys. Intermetallics. 93, 269-273.
DOI: http://dx.doi.org/10.1016/j.intermet.2017.10.004

[5] Ferrari, A., Körmann, F., 2020. Surface segregation in Cr-Mn-Fe-Co-Ni high entropy alloys. Applied Surface Science. 533, 147471.
DOI: https://doi.org/10.1016/j.apsusc.2020.147471

[6] Wilson, P., Field, R., Kaufman, M., 2016. The use of

diffusion multiples to examine the compositional dependence of phase stability and hardness of the Co-Cr-Fe-Mn-Ni high entropy alloy system. Intermetallics. 75, 15-24.
DOI: http://dx.doi.org/10.1016/j.intermet.2016.04.007

[7] Do, H.S., Choi, W.M., Lee, B.J., 2022. A thermodynamic description for the Co-Cr-Fe-Mn-Ni system. Metals and Corrosion. 57, 1373-1389. https://link.springer.com/article/10.1007/s10853-021-06604-8.

[8] Kawamura, M., Asakura, M., Okamoto, N.L., et al., 2021. Plastic deformation of single crystals of the equiatomic Cr−Mn−Fe−Co−Ni high-entropy alloy in tension and compression from 10 K to 1273 K. Acta Materialia. 203, 116454.
DOI: https://doi.org/10.1016/j.actamat.2020.10.073

[9] Osintsev, K., Konovalov, S., Zaguliaev, D., et al., 2022. Investigation of Co-Cr-Fe-Mn-Ni non-equiatomic high-entropy alloy fabricated by wire arc additive manufacturing. Metals. 12, 197.
DOI: https://doi.org/10.3390/met12020197

[10] Hu, M., Cao, Q.P., Wang, X.D., et al., 2022. Tuning nanostructure and mechanical property of Fe−Co−Ni−Cr−Mn high-entropy alloy thin films by substrate temperature. Metals. 12, 197.
DOI: https://doi.org/10.1016/j.mtnano.2021.100130

[11] Mehranpour, M.S., Shahmir, H., Nili-ahmadabadi, M., 2021. Precipitation kinetics in heavily deformed CoCrFeNiMn high entropy alloy. Materials Letters. 288, 129359.
DOI: https://doi.org/10.1016/j.matlet.2021.129359

[12] Xiao, H., Zeng, Q., Xia, L., et al., 2022. Hydrogen-assisted fatigue crack propagation behavior of equiatomic Co-Cr-Fe-Mn-Ni high-entropy alloy. Materials and Corrosion. 73, 550-557.
DOI: https://doi.org/10.1002/maco.202112866

[13] Kim, Y.K., Joo, Y.A., Kim, H.S., et al., 2018. High temperature oxidation behavior of Cr-Mn-Fe-Co-Ni high entropy alloy. Intermetallics. 98, 45-53.
DOI: https://doi.org/10.1016/j.intermet.2018.04.006

[14] Zhu, Z.G., Ma, K.H., Yang, X., et al., 2017. Annealing effect on the phase stability and mechanical properties of (FeNiCrMn)(100-x)Cox high entropy alloys. Journal of Alloys and Compounds. 695, 2945-2950.
DOI: http://dx.doi.org/10.1016/j.jallcom.2016.11.376

[15] Dong, J., Feng, X., Hao, X., et al., 2021. The environmental degradation behavior of FeNiMnCr high entropy alloy in high temperature hydrogenated water. Scripta Materialia. 204, 114127.
DOI: https://doi.org/10.1016/j.scriptamat.2021.114127

[16] Zhang, C., Zhang, F., Jin, K., et al., 2017. Understanding of the elemental diffusion behavior in concentrated solid solution alloys. Journal of Phase Equilibria and Diffusion. 38, 434-444.
DOI: https://doi.org/10.1007/s11669-017-0580-5

[17] Bracq, G., Laurent-Brocq, M., Varvenne, C., et al., 2019. Combining experiments and modeling to explore the solid solution strengthening of high and medium entropy alloys. Acta Materialia. 177, 266-279.
DOI: https://doi.org/10.1016/j.actamat.2019.06.050

[18] Szklarza, Z., Lekki, J., Bobrowski, P., et al., 2018. The effect of SiC nanoparticles addition on the electrochemical response of mechanically alloyed CoCrFeMnNi high entropy alloy. Materials Chemistry and Physics. 215, 385-392.
DOI: https://doi.org/10.1016/j.matchemphys.2018.05.056

[19] Berthod, P., Bernard, J.L., Liébaut, C., 2001. Cobalt-chromium alloy for spinner cups in manufacture of mineral wool from silicate glass. International Patent, PCT International Applications. WO 2001090429 A1 20011129.

[20] Michon, S., Aranda, L., Berthod, P., et al., 2004. High temperature evolution of the microstructure of a cast cobalt base superalloy-Consequences on its thermomechanical properties. Metallurgical Science and Technology. 101, 651-662.
DOI: https://doi.org/10.1051/metal:2004116

[21] Berthod, P., Aranda, L., Vébert, C., et al., 2004. Experimental and thermodynamic study of the high temperature microstructure of tantalum containing nickel-based alloys. Calphad. 28, 159-166.
DOI: https://doi.org/10.1016/j.calphad.2004.07.005

[22] Michon, S., Berthod, P., Aranda, L., et al., 2003. Application of thermodynamic calculations to study high temperature behavior of TaC-strengthened Co-base superalloys. Calphad. 27, 289-294.
DOI: https://doi.org/10.1016/j.calphad.2003.12.003

[23] Berthod, P., Hamini, Y., Aranda, L., et al., 2007. Experimental and thermodynamic study of tantalum-containing iron-based alloys reinforced by carbides: Part I — Case of (Fe, Cr)-based ferritic steels. Calphad. 31, 351-360.
DOI: https://doi.org/10.1016/j.calphad.2007.01.007

[24] Berthod, P., Aranda, L., Hamini, Y., et al., 2007. Experimental and thermodynamic study of tantalum-containing iron-based alloys reinforced by carbides: Part II — Case of (Fe, Ni, Cr)-base austenitic steels. Calphad. 31, 361-369.
DOI: https://doi.org/10.1016/j.calphad.2007.01.008

[25] Berthod, P., Corona, L., 2017. Thermodynamic and experimental study of 30 wt-%Cr-containing {Co, Fe or Ni}-based alloys with very high contents in Ta and C. Canadian Metallurgical Quarterly. 56, 113-122.
DOI: http://dx.doi.org/10.1080/00084433.2016.1267298